Journal of Electronic Materials (2023) 52:7785–7793
https://doi.org/10.1007/s11664-023-10699-x

ORIGINAL RESEARCH ARTICLE

Thermodynamic Assessment of the Fe-Cr-B Ternary System and the Fe-Nd-B-Cr Quaternary System in the Fe-Rich Corner

G. J. Zhou[1] · **A. H. Cai**[1]

Received: 20 July 2023 / Accepted: 23 August 2023 / Published online: 13 September 2023

Abstract

A thermodynamic description for the Fe-Nd-B-Cr quaternary system has been developed on the basis of six constituent binary systems and four critical ternary systems using the CALPHAD (CALculation of PHAse Diagrams) method, which is based on the fact that a phase diagram is a representation of the thermodynamic properties of a system. The Fe-B binary system is modified, and Fe-Nd-Cr and Fe-Cr-B ternary systems are thermodynamically reassessed in order to obtain more reasonable thermodynamic parameters and more accurate phase relations. The assessment results for the Fe-Nd-Cr and Fe-Cr-B ternary systems are in good agreement with the available experimental phase relations, including the liquidus surface projection and the vertical sections, while for the other two ternary systems, the B-Nd-Cr and the Fe-Nd-B systems, the thermodynamic parameters are mainly adopted from optimization results reported in the literature, with slight modifications for the compatibility of all the constituent binary systems. Based on the metastable experimental information, a reasonable, self-consistent, and comprehensive thermodynamic description of the Fe-Nd-B-Cr quaternary system is developed, which is of interest for electronic and magnet materials. The developed thermodynamic description can be further extended as a thermodynamic database for permanent magnet alloy design.

Keywords Magnetic materials · phase diagrams · thermodynamics · Fe-Nd-B-Cr

Introduction

Among commercial permanent magnets, the maximum-energy product magnets of Nd-Fe-B permanent magnet alloys have attracted extensive attention.[1–4] However, the reported magnetic properties of the Nd-Fe-B nanocomposite magnets are not yet satisfactory, mainly due to their relatively low coercivity. Several efforts have been made in the past to improve the coercivity of Nd-Fe-B nanocomposite magnets through the addition of various elements such as Cr or V. [5–11] For example, Suzuki et al.[12] investigated melt-spun $Nd_5Fe_{77-x}Cr_xB_{18}$ ($x = 0$, 3 and 5) alloys. Amorphous $Nd_5Fe_{72}Cr_5B_{18}$ crystallizes into $Fe_3B/Nd_2Fe_{14}B$, regardless of the heating rate, and thus high coercivity values > 300 kA/m are obtained at a wide range of heating rates. Uehara et al.[13] found that the addition of Cr was very effective in improving the hard magnetic characteristics of $Nd_xFe8_{2-x}B_{18}$ ($x = 3.5$ to 5.5) nanocomposites. Gu et al.[14] investigated the influence of the substitution of Cr for Fe on the magnetic properties of $Nd_4Fe_{77.5}B_{18.5}$ alloys. For the alloys with Cr content $x \leq 0.1$, the magnetization and coercivity decreased with increasing Cr content. However, the magnetization and coercivity increased in alloys with $x > 0.1$, as the Cr content increased. It was found that the substitution of Cr for Fe could result in a substantial increase in coercivity from 3 kOe for $Nd_4Fe_{77.5}B_{18.5}$ to 4.9 kOe for $Nd_4(Fe_{0.75}Cr_{0.25})_{77.5}B_{18.5}$ alloys. Shima et al.[15] investigated the influence of a Cr underlayer on the structure and magnetic properties of Nd–Fe–B thin films, and a high coercive force (Hc = 3.7 kOe) was achieved.

From a kinetics point of view, Suzuki et al.[12] investigated the effect of the heating rate on the decomposition process of amorphous $Nd_5Fe_{77-x}Cr_xB_{18}$ ($x = 0$, 3,5) and proposed that Cr played a primary role in the $Nd_5Fe_{74}Cr_3B_{18}$ alloy through retardation of the formation kinetics of $Fe_{23}Nd_2B_3$. Suzuki et al.[12] suggested that Cr may increase the activation free energy for the formation of $Fe_3B/Fe_{23}Nd_2B_3$, and consequently, the Cr-induced formation of $Fe_{14}Nd_2B$ is likely to originate from an increase in ΔG_a^1(where ΔG_a^1 reflects the thermal activation

✉ G. J. Zhou
87973108@qq.com

[1] College of Mechanical Engineering, Hunan Institute of Science and Technology, Yueyang 414000, China

required for the nucleation and growth of $Fe_3B/Fe_{23}Nd_2B_3$ in the amorphous matrix) due to the addition of Cr. From a thermodynamics point of view, Uehara et al.[13] and Sano et al.[16] reported that the high coercivity in the Cr-doped systems was explained by the decrease in the free energy level of the product mixture due to the preferential partitioning of Cr into the Fe_3B phase. They also proposed a schematic diagram to show the relative magnitude of the change in free energy upon crystallization from an amorphous state.

Since the equilibrium experimental information on the Fe-Nd-B-Cr quaternary system is limited, further experimental investigation is necessary for the Cr-containing Fe-Nd-B system. The well-established equilibrium phase diagram can be used to better analyze the metastable solidification process and metastable phase transformations. The purpose of the present study is to evaluate the Fe-Nd-B-Cr quaternary system and to obtain a precise thermodynamic description of the system via the CALPHAD (CAlculation of PHAse Diagrams) approach to guide future microstructural designs of Fe-Nd-B-Cr systems.

Experimental Information

Evaluating the thermodynamics of the Fe-Nd-B-Cr quaternary system requires the evaluation of six binary and four ternary systems. The thermodynamics of the pure elements are described by Dinsdale according to the Scientific Group Thermodata Europe (SGTE),[17] where the free energy of each element is defined with respect to its stable state at 298.15 K and 1 atm. The thermodynamic assessments of Fe-Cr,[18] Cr-B,[19] Fe-B,[20,21] Fe-Nd,[22] B-Nd,[22] and Cr-Nd[20] binary systems were accepted directly in the present work, and the thermodynamic parameters of the Fe-Nd-B system were adopted from Zhou et al.[20] Therefore, the thermodynamic parameters of $Fe_{14}Nd_2B$, Fe_4NdB_4, $Fe_2Nd_5B_6$, $Fe_{23}Nd_2B_3$, and $Fe_{17}Nd_2B$ phases need to be revised to fit the experimental data.

The thermodynamic description of the B-Nd-Cr system reported by Zhou et al.[23] was modified to maintain the compatibility of the thermodynamic models of the binary subsystems. The Fe-Cr-B and Fe-Nd-Cr system are optimized in the present work. A critical review of the data available on the quaternary system is presented and used for the extension of the description of these ternary phases into the quaternary.

Thermodynamic Modeling

Solution Phase

The Gibbs energies of all the solution phases in the Fe-Nd-B-Cr system, including Bcc, Fcc, Hcp, and Dhcp, are expressed as follows:

$$G^{\varphi} = \sum_i x_i {}^0G_i^{\varphi} + \mathrm{RT}\sum_i x_i \ln(x_i) + {}^{\mathrm{ex}}G^{\varphi} + {}^{\mathrm{mg}}G_m^{\varphi} \tag{1}$$

where ${}^0G_i^{\varphi}$ is the Gibbs energy of phase φ of pure component i, x_i is the mole percentage content of i, and ${}^{\mathrm{ex}}G^{\varphi}$ is the excess Gibbs energy of the solution phase, which is expressed as a Redlich–Kister polynomial:

$$\begin{aligned} {}^{\mathrm{ex}}G^{\varphi} = &\sum_i \sum_{j\neq i} x_i x_j L_{i,j} + \sum_i \sum_{j\neq i} \sum_{k\neq j} x_i x_j x_k L_{i,j,k} \\ &+ \sum_i \sum_{j\neq i} \sum_{k\neq j} \sum_{l\neq k} x_i x_j x_k x_l L_{i,j,k,l} \end{aligned} \tag{2}$$

The interaction parameters $L_{i,j}^{\varphi}$ and $L_{i,j,k}^{\varphi}$ of (2) are expressed as

$$L_{i,j}^{\varphi} = a + bT \tag{3}$$

$$L_{i,j,k}^{\varphi} = A + BT \tag{4}$$

$$L_{i,j,k,l}^{\varphi} = A\prime + B\prime T \tag{5}$$

where a, b, A, B, $A\prime$, and $B\prime$ are optimization variables. As the experimental data of the ternary and quaternary solution phases are limited, all the interaction parameters of the ternary and quaternary solution phases are set to 0. ${}^{\mathrm{mg}}G_m^{\varphi}$ is the contribution of magnetism to the Gibbs energies.

Compound Phase

Because of the lack of reliable solubility range experimental data and hot melt data, all intermediate compound phases in the Fe-Nd-B-Cr system deal with stoichiometric phases, and the Gibbs energies of these phase are expressed as the Neumann–Kopp rule (J/mol of atoms):

$$\Delta_f G^0(\varphi) = A + BT + {}^{\mathrm{mg}}G_m \tag{6}$$

where A and B are the parameters to be optimized, and ${}^{\mathrm{mg}}G_m$ is the contribution of magnetism to the Gibbs energies.

Secondly, the research results[24] indicate that Cr exists in a certain soluble form in the Fe-B compounds, and Fe exists in soluble form in the Cr-B compounds. For the Fe-B (or Cr-B) binary system containing a certain soluble form of the third component Cr (or Fe), the Gibbs energy model should be adjusted as follows:

$$\begin{aligned} G^{(\mathrm{Cr,Fe})_x B_y} = &Y_{\mathrm{Cr}}^I G_{\mathrm{Cr}:B}^{(\mathrm{Cr,Fe})_x B_y} + Y_{\mathrm{Fe}}^I G_{\mathrm{Fe},B}^{(\mathrm{Cr,Fe})_x B_y} \\ &+ \frac{x}{x+y} RT(Y_{\mathrm{Cr}}^I \ln Y_{\mathrm{Cr}}^I + Y_{\mathrm{Fe}}^I \ln Y_{\mathrm{Fe}}^I) + Y_{\mathrm{Cr}}^I Y_{\mathrm{Fe}}^I L_{\mathrm{Cr,Fe}:B}^{(\mathrm{Cr,Fe})_x B_y} \end{aligned} \tag{7}$$

where y^I_{Cr} and y^I_{Fe} are the mole fractions of Cr and Fe in the first sublattice.

$L^{(Cr,Fe)_xB_y}_{Cr,Fe:B}$ represent the interaction parameters between Cr and Fe, which are functions of composition and temperature, expressed as the Redlich–Kister polynomial:

$$L^{(Cr,Fe)_xB_y}_{Cr,Fe:B} = A + BT \tag{8}$$

where A and B are the parameters to be optimized.

The binary phase FeB, Fe_2B, and Fe_3B of Fe-B contain certain solubility of the third component Cr, $G^{(Cr,Fe)_xB_y}_{Fe:B}$ derived from the Fe-B binary system:

$$G^{(Cr,Fe)_xB_y}_{Fe:B} = G^{Fe_xB_y}_{Fe:B} \tag{9}$$

$G^{(Cr,Fe)_xB_y}_{Cr:B}$ is the Gibbs energy of the hypothetical compounds Cr_xB_y.

$$G^{(Cr,Fe)_xB_y}_{Cr:B} = \frac{x}{x+y}{}^0G^{Bcc}_{Cr} + \frac{y}{x+y}{}^0G^{\beta}_{B} + A + BT \tag{10}$$

where A and B are the parameters to be optimized.

Similarly, the binary phase Cr_2B, Cr_5B_3, CrB, Cr_3B_4, CrB_2, and CrB_4 of Cr-B contain certainly solubility of the third component Fe, $G^{(Cr,Fe)_xB_y}_{Cr:B}$ derived from the Cr-B binary system:

$$G^{(Cr,Fe)_xB_y}_{Cr:B} = G^{Cr_xB_y}_{Cr:B} \tag{11}$$

$G^{(Cr,Fe)_xB_y}_{Fe:B}$ is the Gibbs energy of the hypothetical compounds Fe_xB_y

$$G^{(Cr,Fe)_xB_y}_{Fe:B} = \frac{x}{x+y}{}^0G^{Bcc}_{Fe} + \frac{y}{x+y}{}^0G^{\beta}_{B} + A + BT \tag{12}$$

where A and B are the parameters to be optimized.

Results and Discussion

The optimization was carried out using Thermo-Calc software, which can handle various kinds of experimental data. The thermodynamic parameters of the Fe-Nd-B-Cr quaternary system developed in this study are outlined in Table I.

The Fe-B System

To fit the Fe-Cr-B ternary system, we re-modified the Fe-B binary system thermodynamic parameters, and the enthalpy of formation at 298 K in the Fe-B system was calculated as shown in Fig. 1. Because Fe_3B is a metastable phase, the enthalpy of formation should be slightly positive, and the data should be slightly adjusted, as the initial value of parameter A to be optimized in the Gibbs free energy expression of the Fe_3B metastable phase. We obtained the thermodynamic parameters of the Fe_3B phase by calculating the reaction temperature of the metastable eutectic reaction Liq $\rightarrow Fe_3B + \gamma - Fe$. The calculated phase diagram is shown in Fig. 2, which includes the equilibrium phase (black line) and metastable phase (red line). It should be noted that a small upward inflection point on the curve is observed at the position of the Fe_3B phase, but this is consistent with the fact that the Fe_3B phase is a metastable phase.[21]

Reassessment of Fe-Cr-B Ternary Systems

Based on the optimized thermodynamic parameters, the set of experimental data for stable equilibrium of the Fe-Cr-B system were calculated. For this purpose, the experimental data reported by Uehara et al.[13] were used in the optimization.

The calculated equilibrium phase diagrams compared with experimental phase diagrams are shown in Figs. 3 and 4. The results show good agreement except for the composition of the Cr_2B phase in the $CrB + Cr_5B_3 + Cr_2B$ three-phase equilibrium. Because the amount of Cr added to the Fe-Nd-B alloy is small, and it is sufficient to consider only 5 at.% Cr in the Fe-Nd-B-Cr system, this difference will have little effect on the Cr-poor corner of the Fe-Nd-B-Cr system.

Taking no account of the Fe_2B equilibrium phase, the calculated metastable isothermal cross-section of the Fe-Cr-B ternary system at 953 K is shown in Fig. 5. The solubility of Cr in the Fe_3B metastable phase is calculated to be 4.26 at.%, which is consistent with the data measured by Uehara et al.[13] at 4.26 at.%.

The liquid phase projection diagram of the Fe-Cr-B ternary system is calculated as shown in Fig. 6, which includes eight invariant reactions related to the liquid phase as shown in Table II.

Reassessment of Fe-Nd-Cr Ternary Systems

Experimental data for the Fe-Cr-Nd system are limited, and as there are no literature data available to represent the liquid surface, in this work the Fe-Cr, Fe-Nd, and Cr-Nd binary systems are combined to extrapolate the Fe-Cr-Nd ternary system. Figure 7 shows the liquidus projection of the Fe-Cr-Nd system, and the invariant reactions in the Fe-Cr-Nd system are shown in Table III.

The Fe-Nd-B-Cr Quaternary System

The thermodynamics of the Fe-Nd-B-Cr quaternary system in the Fe-rich corner are assessed by the combination of four ternary and six binary systems mentioned above, as illustrated in Fig. 8.

Table I Thermodynamic parameters of the Fe-Nd-B-Cr quaternary system

Phase	Thermodynamic parameters (J/mol of atoms)	References
Liquid	${}^{0}L^{\text{Liquid}}_{\text{B, Fe}}=-133438+33.95\times \text{T}$	26
	${}^{1}L^{\text{Liquid}}_{\text{B, Fe}}=7771$	26
	${}^{2}L^{\text{Liquid}}_{\text{B, Fe}}=29739$	26
	${}^{0}L^{\text{Liquid}}_{\text{Fe,Nd}}=3221$	22
	${}^{1}L^{\text{Liquid}}_{\text{Fe, Nd}}=6216$	22
	${}^{2}L^{\text{Liquid}}_{\text{Fe, Nd}}=4826$	22
	${}^{0}L^{\text{Liquid}}_{\text{B, Nd}}=-100000+30.37\times T$	This work
	${}^{1}L^{\text{Liquid}}_{\text{B, Nd}}=-25059.7$	This work
	${}^{0}L^{\text{Liquid}}_{\text{Cr, Nd}}=37262.8-0.81\times \text{T}$	This work
	${}^{0}L^{\text{Liquid}}_{\text{Cr, Nd}}=20582.2-6.37\times T$	This work
	${}^{0}L^{\text{Liquid}}_{\text{B, Cr}}=-165600+34\times T$	27
	${}^{1}L^{\text{Liquid}}_{\text{B, Cr}}=-10000$	27
	${}^{2}L^{\text{Liquid}}_{\text{B, Cr}}=20000$	27
	${}^{0}L^{\text{Liquid}}_{\text{Cr, Fe}}=-14550+6.65\times T$	18
Bcc	${}^{0}L^{\text{Bcc}}_{B, \text{Fe}}=-47920+42.09\times T$	26
	${}^{0}L^{\text{Bcc}}_{\text{Fe, Nd}}=50562-4.970\times T$	22
	${}^{1}L^{\text{Bcc}}_{\text{Fe, Nd}}=-38667+19.10\times T$	22
	${}^{0}L^{\text{Bcc}}_{\text{Cr, Nd}}=48175.5-0.555\times T$	This work
	${}^{0}L^{\text{Bcc}}_{B, \text{Cr}}=-140000+49\times T$	27
	${}^{0}L^{\text{Bcc}}_{\text{Cr, Fe}}=20500-9.68\times T$	18
	${}^{0}T^{\text{Bcc}}_{c\ \text{Cr, Fe}}=1650$	18
	${}^{0}\beta^{\text{Bcc}}_{\text{Cr, Fe}}=-0.85$	18
	${}^{1}T^{\text{Bcc}}_{c\ \text{Cr, Fe}}=550$	18
Fcc	${}^{0}L^{\text{Fcc}}_{B, \text{Fe}}=-62952+49.90\times T$	27
	${}^{0}L^{\text{Fcc}}_{\text{Fe, Nd}}=35356-2.962\times T$	22
	${}^{0}L^{\text{Fcc}}_{\text{Cr, Fe}}=10833-7.477\times T$	18
	${}^{1}L^{\text{Fcc}}_{\text{Cr, Fe}}=1410$	18
	${}^{0}L^{\text{Fcc}}_{\text{Cr, Nd}}=20000$	This work
FeB	$G^{\text{FeB}}_{\text{Fe:}B}=0.5{}^{0}G^{\text{Bcc}}_{\text{Fe}}+0.5{}^{0}G^{\beta}_{B}-35287+5.992\times \text{T}$	26
	$G^{\text{FeB}}_{\text{Cr:B}}=0.5{}^{0}G^{\text{Bcc}}_{\text{Cr}}+0.5{}^{0}G^{\beta}_{\text{B}}-44908+4.00\times T$	This work
	${}^{0}L^{\text{FeB}}_{\text{Cr, Fe:B}}=6000$	This work
Fe_2B	$G^{\text{Fe}_2\text{B}}_{\text{Fe:B}}=0.6667{}^{0}G^{\text{Bcc}}_{\text{Fe}}+0.3333{}^{0}G^{\beta}_{\text{B}}-26261+3.466\times T$	27
	$G^{\text{Fe}_2\text{B}}_{\text{Cr:B}}=0.6667{}^{0}G^{\text{Bcc}}_{\text{Cr}}+0.3333{}^{0}G^{\beta}_{\text{B}}-37450+4\times T$	This work
	${}^{0}T^{\text{Fe}_2\text{B}}_{\text{c Cr, Fe:B}}=-1622$	27
	${}^{0}\beta^{\text{Fe}_2\text{B}}_{\text{Cr, Fe:B}}=-4.007$	27
	${}^{1}T^{\text{Fe}_2\text{B}}_{\text{c Cr, Fe:B}}=3150$	27
	${}^{1}\beta^{\text{Fe}_2\text{B}}_{\text{Cr, Fe:B}}=-1.1926$	27
	${}^{2}T^{\text{Fe}_2\text{B}}_{\text{c Cr, Fe:B}}=3269$	27
	${}^{2}\beta^{\text{Fe}_2\text{B}}_{\text{Cr, Fe:B}}=0.1828$	27
Fe_3B	$G^{\text{Fe}_3\text{B}}_{\text{Fe:B}}=0.75{}^{0}G^{\text{Bcc}}_{\text{Fe}}+0.25{}^{0}G^{\beta}_{\text{B}}-21732.45+4.6322\times T$	This work
	$G^{\text{Fe}_3\text{B}}_{\text{Cr:B}}=0.75{}^{0}G^{\text{Bcc}}_{\text{Cr}}+0.25{}^{0}G^{\beta}_{\text{B}}-20000+10.6322\times T$	This work
	${}^{0}L^{\text{Fe}_3\text{B}}_{\text{Cr, Fe:B}}=-10000$	This work
CrB	$G^{\text{CrB}}_{\text{Cr:B}}=0.5{}^{0}G^{\text{Bcc}}_{\text{Cr}}+0.5{}^{0}G^{\beta}_{\text{B}}-47608+4.86\times T$	27
	$G^{\text{CrB}}_{\text{Fe:B}}=0.5{}^{0}G^{\text{Bcc}}_{\text{Fe}}+0.5{}^{0}G^{\beta}_{\text{B}}-30500+6.35\times T$	This work
	${}^{0}L^{\text{CrB}}_{\text{Cr, Fe:B}}=2000$	This work

Table I (continued)

Phase	Thermodynamic parameters (J/mol of atoms)	References
Cr_2B	$G^{Cr_2B}_{Cr:B} = 0.6667\,{}^0G^{Bcc}_{Cr} + 0.3333\,{}^0G^{\beta}_{B} - 22161 + 3.466 \times T$	27
	$G^{Cr_2B}_{Fe:B} = 0.6667\,{}^0G^{Bcc}_{Fe} + 0.3333\,{}^0G^{\beta}_{B} - 37675 + 4 \times T$	This work
	${}^0L^{Cr_2B}_{Cr,\,Fe:B} = -12500$	This work
Cr_3B_4	$G^{Cr_3B_4}_{Cr:B} = 0.4286\,{}^0G^{Bcc}_{Cr} + 0.5714\,{}^0G^{\beta}_{B} - 44750 + 4 \times T$	27
	$G^{Cr_3B_4}_{Fe:B} = 0.4286\,{}^0G^{Bcc}_{Fe} + 0.5714\,{}^0G^{\beta}_{B} - 25000 + 4 \times T$	This work
Cr_5B_3	$G^{Cr_5B_3}_{Cr:B} = 0.6250\,{}^0G^{Bcc}_{Cr} + 0.3750\,{}^0G^{\beta}_{B} - 40300 + 4.15 \times T$	27
	$G^{Cr_5B_3}_{Fe:B} = 0.6250\,{}^0G^{Bcc}_{Fe} + 0.3750\,{}^0G^{\beta}_{B} - 25000 + 4.15 \times T$	This work
	${}^0L^{Cr_5B_3}_{Cr,\,Fe:B} = -5000$	This work
CrB_2	$G^{CrB_2}_{Cr:B} = 0.3333\,{}^0G^{Bcc}_{Cr} + 0.6667\,{}^0G^{\beta}_{B} - 38000 + 1.75 \times T$	27
	$G^{CrB_2}_{Fe:B} = 0.3333\,{}^0G^{Bcc}_{Fe} + 0.6667\,{}^0G^{\beta}_{B} - 15000 + 4 \times T$	This work
CrB_4	$G^{CrB_4}_{Cr:B} = 0.2\,{}^0G^{Bcc}_{Cr} + 0.8\,{}^0G^{\beta}_{B} - 25000 + 2.279 \times T$	27
	$G^{CrB_4}_{Fe:B} = 0.2\,{}^0G^{Bcc}_{Fe} + 0.8\,{}^0G^{\beta}_{B} - 10000 + 3 \times T$	This work
Nd_2B_5	$G^{Nd_2B_5}_{Nd:B} = 0.2857\,{}^0G^{Dhcp}_{Nd} + 0.7143\,{}^0G^{\beta}_{B} - 62800 + 13.64 \times T$	This work
NdB_4	$G^{NdB_4}_{Nd:B} = 0.2\,{}^0G^{Dhcp}_{Nd} + 0.8\,{}^0G^{\beta}_{B} - 70500 + 16.04 \times T$	This work
NdB_6	$G^{NdB_6}_{Nd:B} = 0.1429\,{}^0G^{Dhcp}_{Nd} + 0.8571\,{}^0G^{\beta}_{B} - 60440 + 12.23 \times T$	This work
NdB_{66}	$G^{NdB_{66}}_{Nd:B} = 0.02\,{}^0G^{Dhcp}_{Nd} + 0.98\,{}^0G^{\beta}_{B} - 8306 + 1.074 \times T$	This work
$Fe_{17}Nd_2$	$G^{Fe_{17}Nd_2}_{Fe:Nd} = 0.8947\,{}^0G^{Bcc}_{Fe} + 0.1053\,{}^0G^{Dhcp}_{Nd} - 7385 + 3.6 \times T$	22
	$T^{Fe_{17}Nd_2}_{c\,Fe:Nd} = 327$	22
	$\beta^{Fe_{17}Nd_2}_{Fe:Nd} = 2.3$	22
$Fe_{17}Nd_5$	$G^{Fe_{17}Nd_5}_{Fe:Nd} = 0.7727\,{}^0G^{Bcc}_{Fe} + 0.2273\,{}^0G^{Dhcp}_{Nd} 6175 - 2.698 \times T$	22
	$T^{Fe_{17}Nd_5}_{c\,Fe:Nd} = 503$	22
	$\beta^{Fe_{17}Nd_5}_{Fe:Nd} = 2.3$	22
σ	$G^{\sigma}_{Fe:Cr:Cr} = 0.2667\,{}^0G^{Fcc}_{Fe} + 0.7333\,{}^0G^{Bcc}_{Cr} + 3076.67 - 3.2 \times T$	18
	$G^{\sigma}_{Fe:Cr:Fe} = 0.2667\,{}^0G^{Fcc}_{Fe} + 0.1333\,{}^0G^{Bcc}_{Cr} + 0.6000\,{}^0G^{Bcc}_{Fe} + 3910 - 3.2 \times T$	18
B_4NdCr	$G^{B_4NdCr}_{B:Cr:Nd} = 0.6650\,{}^0G^{\beta}_{B} + 0.1420\,{}^0G^{Bcc}_{Cr} + 0.1930\,{}^0G^{Dhcp}_{Nd} - 63050 + 14 \times T$	This work
B_6NdCr_2	$G^{B_6NdCr_2}_{B:Cr:Nd} = 0.6620\,{}^0G^{\beta}_{B} + 0.1860\,{}^0G^{Bcc}_{Cr} + 0.1520\,{}^0G^{Dhcp}_{Nd} - 62050 + 13 \times T$	This work
$Fe_{14}Nd_2B$	$G^{Fe_{14}Nd_2B}_{Fe:Nd:B} = 0.8235\,{}^0G^{Bcc}_{Fe} + 0.1177\,{}^0G^{Dhcp}_{Nd} + 0.0588\,{}^0G^{\beta}_{B} - 11947.4 + 3.278 \times T$	This work
	$T^{Fe_{14}Nd_2B}_{c\,Fe:Nd:B} = 586$	28
	$\beta^{Fe_{14}Nd_2B}_{Fe:Nd:B} = 2.4$	28
Fe_4NdB_4	$G^{Fe_4NdB_4}_{Fe:Nd:B} = 0.4396\,{}^0G^{Bcc}_{Fe} + 0.1208\,{}^0G^{Dhcp}_{Nd} + 0.4396\,{}^0G^{\beta}_{B} - 43698.5 + 8.996 \times T$	This work
	$T^{Fe_4NdB_4}_{c\,Fe:Nd:B} = 10$	28
	$\beta^{Fe_4NdB_4}_{Fe:Nd:B} = 0.2$	28
$Fe_2Nd_5B_6$	$G^{Fe_2Nd_5B_6}_{Fe:Nd:B} = 0.1539\,{}^0G^{Bcc}_{Fe} + 0.3846\,{}^0G^{Dhcp}_{Nd} + 0.4615\,{}^0G^{\beta}_{B} - 42341 + 7.572 \times T$	This work
	$T^{Fe_2Nd_5B_6}_{c\,Fe:Nd:B} = 64$	28
	$\beta^{Fe_2Nd_5B_6}_{Fe:Nd:B} = 0.5$	28
$Fe_{23}Nd_2B_3$	$G^{Fe_{23}Nd_2B_3}_{Fe:Nd:B} = 0.8214\,{}^0G^{Bcc}_{Fe} + 0.0714\,{}^0G^{Dhcp}_{Nd} + 0.1072\,{}^0G^{\beta}_{B} - 15672.2 + 5.388 \times T$	This work
	$T^{Fe_{23}Nd_2B_3}_{c\,Fe:Nd:B} = 655$	29
	$\beta^{Fe_{23}Nd_2B_3}_{Fe:Nd:B} = 1.7$	29
$Fe_{17}Nd_2B$	$G^{Fe_{17}Nd_2B}_{Fe:Nd:B} = 0.85\,{}^0G^{Bcc}_{Fe} + 0.10\,{}^0G^{Dhcp}_{Nd} + 0.05\,{}^0G^{\beta}_{B} - 51.9385 - 3.89558 \times T$	This work

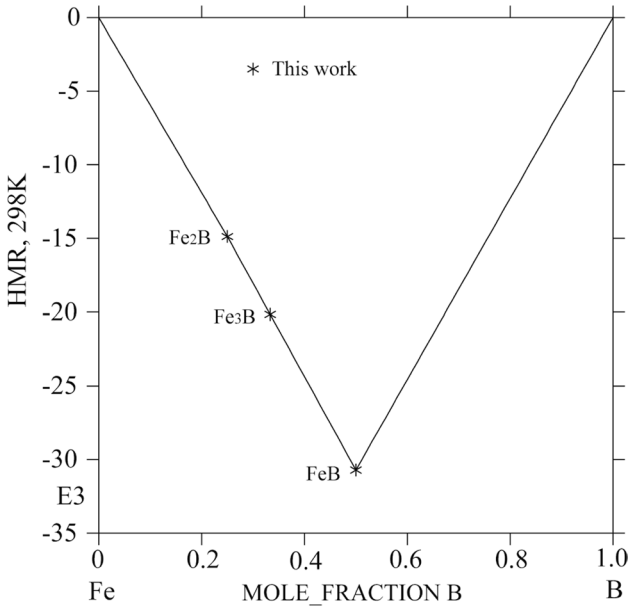

Fig. 1 Calculated enthalpy of formation at 298 K in the Fe-B system.

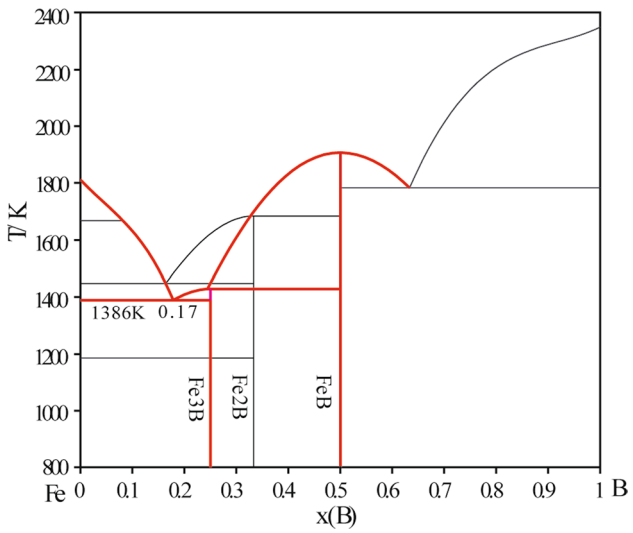

Fig. 2 Calculated Fe-B stable (black line) and metastable (red line) phase diagrams (Color figure online).

The experimental phase diagram and thermodynamic data for the Fe-Nd-B-Cr quaternary system are limited. Uehara et al.[13] reported that less than 0.7 at.% Cr was dissolved in the $Fe_{14}Nd_2B$ phase. Hiroaswa et al.[25] noted that the solubility of Cr in the ternary phases $Fe_{14}Nd_2B$ and Fe_4NdB_4 was very low. In addition, there are no reports on the solubility of Cr in $Fe_2Nd_5B_6$, $Fe_{23}Nd_2B_3$, and $Fe_{17}Nd_2B$ phases. As a consequence, in the present work we do not consider the solubility of Cr in $Fe_{14}Nd_2B$, Fe_4NdB_4, $Fe_2Nd_5B_6$, $Fe_{23}Nd_2B_3$, and $Fe_{17}Nd_2B$ ternary phases.

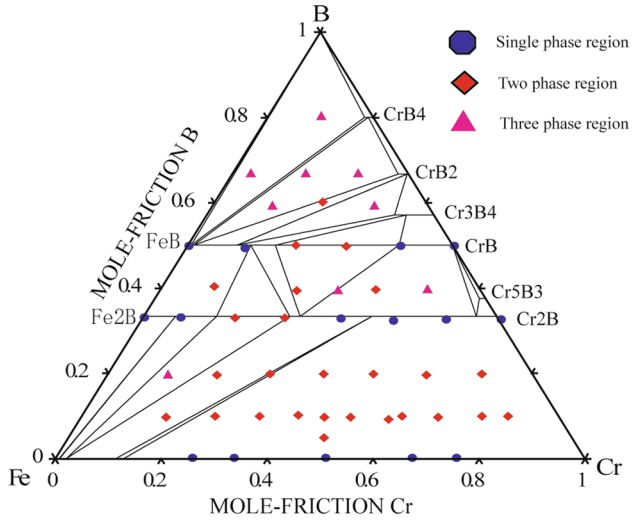

Fig. 3 Comparison between the calculated and experimental phase equlibria in the Fe-Cr-B at 973 K based on reported experimental data.[24]

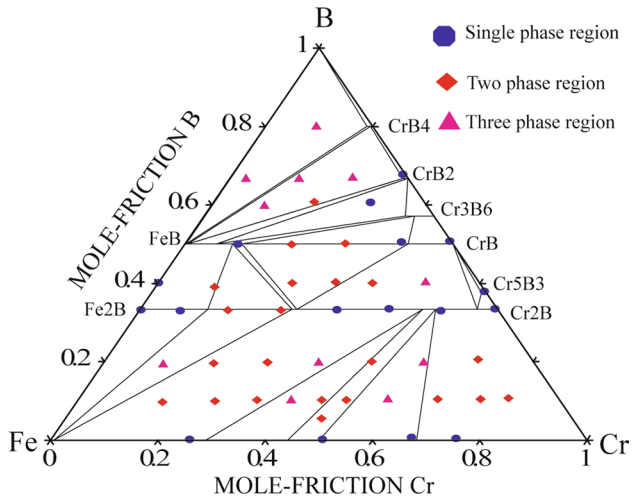

Fig. 4 Comparison between the calculated and experimental phase equlibria in the Fe-Cr-B at 1173 K based on reported experimental data.[24]

Previous research[25] suggests that in Cr-doped Fe-Nd-B nanocomposite magnets, Cr is concentrated in Fe and/or Fe_xB phases and depleted in Fe_4NdB_4 and some of $Fe_{14}Nd_2B$ phases after crystallization. Suzuki et al.[12] examined the changes in the magnetic and structural properties of amorphous $Fe_{74}Cr_3Nd_5B_{18}$ after annealing for periods ranging from 180 s to 605 ks (1 week) at 953 K. We believe that 1 week is sufficient time to reach the equilibrium state. Therefore, based on the experimental results by Suzuki et al.,[12] the equilibrium state of the $Fe_{74}Cr_3Nd_5B_{18}$ alloy should be the three-phase coexistence of $Fe_4NdB_4 + Fe_2B + \alpha$-Fe at 953 K. From the phase diagram

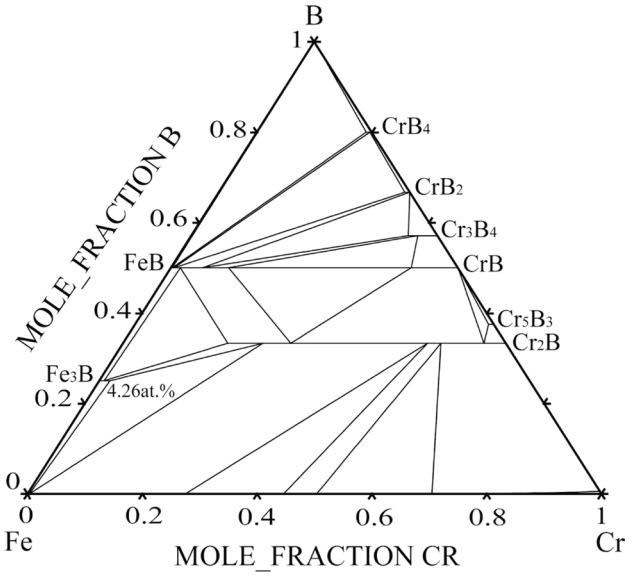

Fig. 5 The calculated metastable isothermal section of Fe-Cr-B at 953 K.

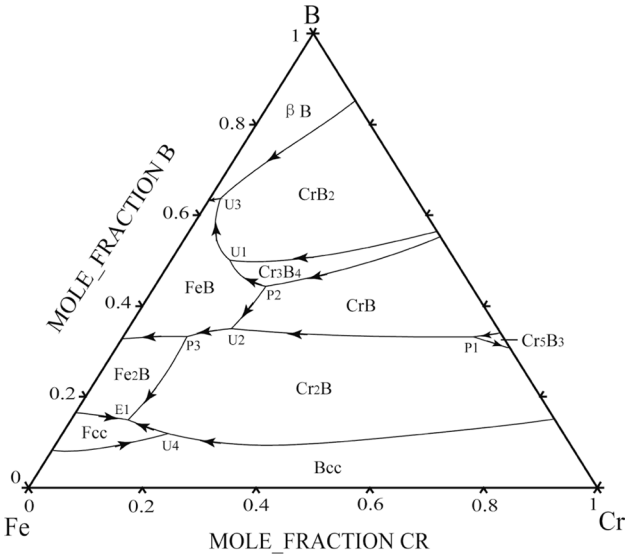

Fig. 6 The calculated liquidus projection of the Fe-Cr-B system.

analysis, the connecting line between Fe_4NdB_4 and α-Fe should be a balanced junction line in the phase diagram at 953 K. In present study, the calculated isothermal section of the Fe-Nd-B-Cr quaternary system (Cr = 3 at.%) at 953 K is shown in Fig. 8. These results indicate that the connecting line between Fe_4NdB_4 and α-Fe is a balanced junction, which is in agreement with the experimental results reported by Suzuki et al.[12]

As shown in Fig. 8, the $Fe_{74}Cr_3Nd_5B_{18}$ alloy is still not present in the $Fe_4NdB_4 + Fe_2B + α$-Fe three-phase region. This is because this state is the nearest equilibrium state but still not the fully equilibrium state. The first crystalline product Fe_3B (which appears after annealing for 180 s) is transformed to Fe_2B (which appears after annealing for 28.8 ks), resulting in the incomplete disappearance of Fe_2B after annealing for 1 week. Suzuki et al.[12] also measured the coercivity change as a function of annealing time for $Fe_{74}Cr_3Nd_5B_{18}$. The coercivity deteriorates dramatically after annealing for 1 week. Our calculation shows that, in equilibrium, $Fe_{74}Cr_3Nd_5B_{18}$ consists of $Fe_4NdB_4 + α$-Fe with a small amount of $Fe_{14}Nd_2B + Cr_2B$. It may be that the intensity of $Fe_{14}Nd_2B$ and Cr_2B is too weak to be detected, so the amount of $Fe_{14}Nd_2B$ is insufficient to improve the coercivity.

The difference is that the composition of the equilibrium phase of the $Fe_{74}Cr_3Nd_5B_{18}$ alloy includes the four phases of $Fe_{14}Nd_2B$ (22.33 at.%) + Fe_4NdB_4 (19.38 at.%) + α-Fe (33.73 at.%) + Fe_2B (24.56 at.%), but the experimental results[12] reflect the three-phase equilibrium of $Fe_4NeB_4 + Fe_2B + α$-Fe. Therefore, the reliability of the experimental results[12] is examined. Firstly, as shown in Fig. 8, the connecting line between Fe_4NdB_4 and α-Fe still has a range that can be changed. If the connecting line is moved by adjusting the thermodynamic parameters, the composition points of the $Fe_{74}Cr_3Nd_5B_{18}$ alloy fall into the three-phase zone of $Fe_4NdB_4 + Fe_2B + α$-Fe. Let us consider the extreme situation, where the connecting line moves to the right only between Fe_4NdB_4 and α-Fe. Additionally, suppose that an artificial line is drawn between Fe_4NdB_4 and α-Fe at an isothermal section of the Fe-Nd-B-Cr quaternary system (Cr = 3 at.%) at 953 K, as shown in Fig. 8

Table II Invariant reactions in the Fe-Cr-B system

Symbol	Reaction	Composition of liquid (at.%)			T(K)	Type
		Fe	Cr	B		
P1	$L + Cr_5B_3 + CrB \leftrightarrow Cr_2B$	5.3	61.6	33.1	2144	Quasi-peritectic
P2	$L + Cr_3B_4 + CrB \leftrightarrow FeB$	36.2	19.5	44.3	2019	Peritectic
U1	$L + Cr_3B_4 \leftrightarrow CrB_2 + FeB$	39.6	10.3	50.1	1957	Quasi-peritectic
U2	$L + CrB \leftrightarrow FeB + Cr_2B$	47.0	18.1	34.9	1848	Quasi-peritectic
U3	$L + CrB_2 \leftrightarrow β\text{-}B + FeB$	34.5	1.9	63.6	1783	Quasi-peritectic
P3	$L + FeB + Cr_2B \leftrightarrow Fe_2B$	55.6	11.2	33.2	1736	Peritectic
U4	$L + Bcc \leftrightarrow Cr_2B + Fcc$	69.6	18.6	11.8	1452	Quasi-peritectic
E1	$L \leftrightarrow Cr_2B + Fe_2B + Fcc$	75.2	10.0	14.8	1424	Eutectic

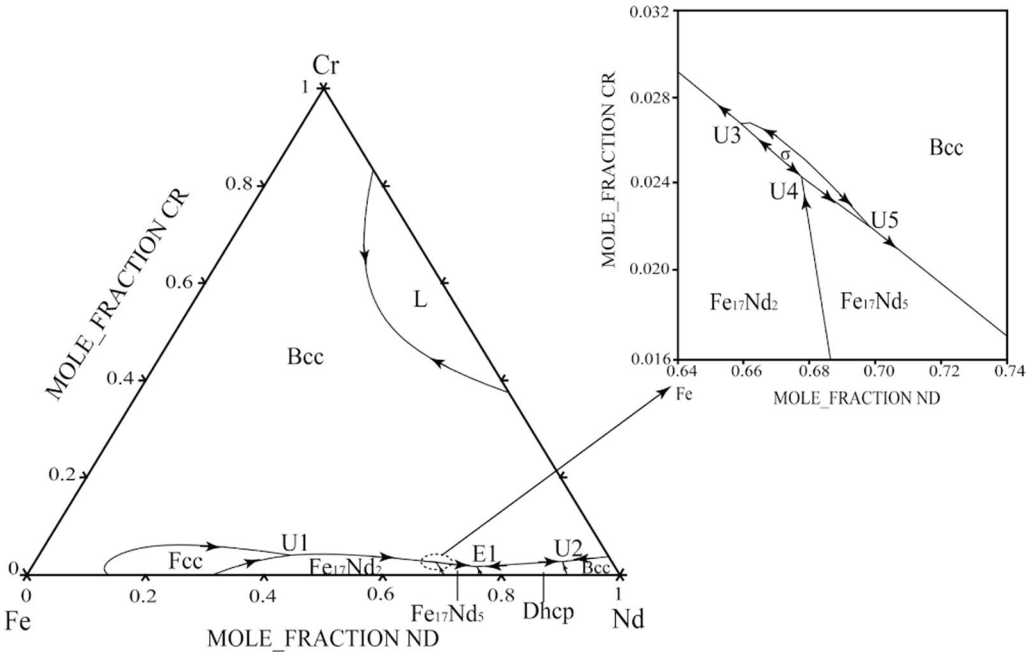

Fig. 7 The calculated liquidus projection of the Fe-Nd-Cr system.

Table III Invariant reactions in the Fe-Nd-Cr system

Symbol	Reaction	Composition of liquid (at.%)			T(K)	Type
		Nd	Fe	Cr		
U1	$L + Fcc \leftrightarrow Bcc + Fe_{17}Nd_2$	42.5	53.6	3.9	1319	Quasi-peritectic
U2	$L + Bcc \leftrightarrow Bcc + Dhcp$	89.0	8.3	2.7	1109	Quasi-peritectic
U3	$L + \sigma \leftrightarrow Bcc + Fe_{17}Nd_2$	65.9	31.4	2.7	1045	Quasi-peritectic
U4	$L + Fe_{17}Nd_2 \leftrightarrow \sigma + Fe_{17}Nd_5$	67.8	29.8	2.4	1023	Quasi-peritectic
U5	$L + \sigma \leftrightarrow Fe_{17}Nd_5 + Bcc$	69.8	28.0	2.2	1000	Quasi-peritectic
E1	$L \leftrightarrow Fe_{17}Nd_5 + Bcc + Dhcp$	75.0	23.4	1.6	942	Eutectic

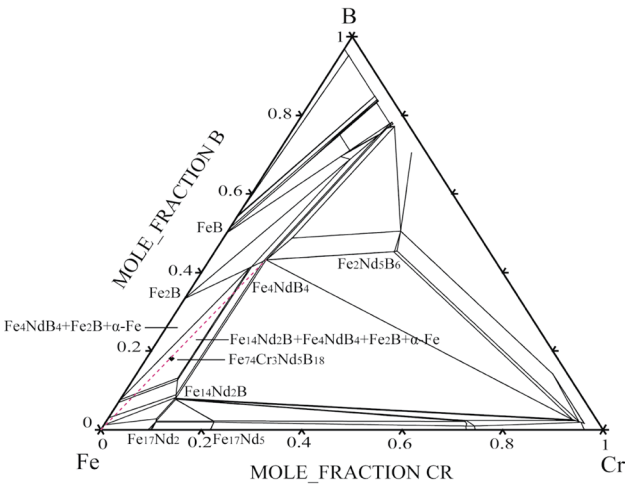

Fig. 8 Calculated isothermal section of Fe-Nd-B-Cr quaternary system (Cr = 3 at.%) at 953 K.

(red dashed line). The $Fe_{74}Cr_3Nd_5B_{18}$ alloy will not fall into the three-phase zone of $Fe_4NdB_4 + Fe_2B + \alpha$-Fe, which indicates that there is some error in the experiment results.[12] It is possible that this error is the result of two factors: (1) in the process of optimization, the limited experimental data causes errors in the interaction parameters, or alternatively, (2) the enhanced oxidation and volatilization promoted by the rare earth element Nd result in experimental deviation between alloy composition and nominal composition. Thus, the present calculation is reasonable, but further experimental verification is still needed.

Conclusions

For the development of the thermodynamic database of the Fe-Nd-B-Cr quaternary system and its four constituent ternary systems, the Fe-Nd-Cr and Fe-Cr-B ternary systems

were thermodynamically reassessed on the basis of previous works to achieve compatibility with all the constituent binary systems. As a result, (1) modifications were performed to the equilibrium Fe-Cr-B ternary system, and in the improved Fe-Nd-B system, metastable phases of Fe_3B and $Fe_{23}Nd_2B_3$ were present. We re-modified the Fe-B binary system thermodynamic parameters, and the enthalpy of formation was calculated at 298 K in the Fe-B system. (2) Six binary systems and four ternary systems were combined to extrapolate the Fe-Nd-B-Cr quaternary system. The framework of the Fe-Nd-B-Cr system in the Fe-rich corner was constructed.

Acknowledgments This work was supported by the Natural Science Foundation of Hunan Province (Grant No. 2020JJ4335).

Conflict of interest The authors declare that they have no known competing financial interests or personal relationships that could have appeared to influence the work reported in this paper.

References

1. X. Fu, H.J. Peng, R.G. Jia, and T. Li, Effect of non-rare-earth element enrichment on in-the-column secondary electron image contrast of Nd-rich phases in Nd-Fe-B sintered magnets. *Mater. Charact.* 23, 113042 (2023).
2. S.H. Dong, X.T. Li, Q.M. Lu, W.Q. Liu, Y.F. Wu, and M. Yue, Study on mechanical properties of recycled sintered Nd-Fe-B magnets. *J. Alloy. Compd.* 962, 171156 (2023).
3. X.S. Xia, G.T. Wei, L. Wu, Y. Ouyang, X. Tang, Y.Y. Du, R.J. Chen, J.Y. Ju, W.Z. Yin, and A. Yan, Improvement of overall texture and magnetic properties in bulk hot-deformed Nd-Fe-B composite magnets by the design of macrostructure. *J. Alloys Compd.* 960, 170759 (2023).
4. M. Liu, L. Zhang, B. Zhao, F. Chen, X. Xia, Y. Yu, H. Yamamoto, and K. Ito, Orientation dependence of plastic deformation of sintered Nd-Fe-B magnets at high temperature. *Acta Mater.* 244, 118559 (2023).
5. W.C. Chang, D.Y. Chiou, S.H. Wu, B.M. Ma, and C.O. Bounds, High performance α-Fe/$Nd_2Fe_{14}Nd_2Fe_{14}B$-type nanocomposites. *Appl. Phys. Lett.* 72, 121 (1998).
6. W.F. Miao, J. Ding, P.G. McCormick, and R. Street, Remanence-enhanced Nd8Fe87M1B4 (M = Fe, V, Si, Ga, Cr) alloys. *J. Magn. Magn. Mater.* 171–181, 976 (1998).
7. J. Jakubowicz, A. Szlaferek, and M. Jurczyk, Magnetic properties of nanostructured Nd 2(Fe Co, Cr) 1 4B/α-Fe magnets. *J. Alloy. Compd.* 283, 307 (1999).
8. J. Jakubowicz, M. Jurczyk, A. Handstein, D. Hinz, O. Gutflfleisch, and K.H. Müller, Temperature dependence of magnetic properties for nanocomposite Nd2(Fe Co, M)14B/α-Fe magnets. *J. Magn. Magn. Mater.* 208, 163 (2000).
9. J. Jakubowicz and M. Giersig, Structure and magnetic properties of Nd2(Fe Co, Al, Cr)14B/α-Fe nanocomposite magnets. *J. Alloys Compd.* 349, 311 (2003).
10. X.F. Ding, Y.J. Wu, L.J. Yang, C. Xu, S. Mao, Y.P. Wang, D. Zheng, and Z.L. Song, The properties of chromium oxide coatings on NdFeB magnets by magnetron sputtering with ion beam assisted deposition. *Vacuum* 131, 127 (2016).
11. J.W. Zheng, M. Ling, and Q.P. Xia, A preparation method and effects of Al-Cr coating on NdFeB sintered magnets. *J. Magn. Magn. Mater.* 324, 3966 (2012).
12. K. Suzuki, J.M. Cadogan, Y. Shigemoto, K. Murakami, T. Miyoshi, and Y. Shioya, Formation and decomposition of Fe3B/Nd2Fe14B nanocomposite structure in Fe-Nd-B-Cr melt-spun ribbons under isothermal annealing. *J. Appl. Phys.* 85, 5914 (1999).
13. M. Uehara, S. Hirosawa, H. Kanekiyo, N. Sano, and T. Tomida, Effect of Cr-doping on crystallization sequence and magnetic properties of Fe3B/Nd2Fe14B nanocomposite permanent magnets. *Nanostruct. Mater.* 10, 151 (1998).
14. B.X. Gu, B.G. Shen, and R.H. Zhai, Influence of substitution of Cr for Fe on magnetic properties of $Nd_4Fe_{77.5}B_{18.5}$ alloys. *JJ Magn Magn. Mater.* 124, 85 (1993).
15. T. Shima, A. Kamegawa, and H. Fujimori, Enhanced coercive force of Nd-Fe-B thin films by the introduction of a Cr underlayer. *J. Alloy. Compd.* 281, 46 (1998).
16. N. Sano, T. Tomida, S. Hirosawa, M. Uehara, and H. Kanekiyo, Crystallization process of a rapidly quenched Fe-B-Nd nanocomposite magnet. *Mater. Sci. Eng. A.* 250(1), 146 (1998).
17. A.T. Dinsdale, SGTE data for pure elements. *Calphad* 15, 317 (1991).
18. J.O. Andersson and B. Sundman, Thermodynamic properties of the Cr-Fe system. *Calphad* 83, 83 (1987).
19. C.E. Campbell and U.R. Kattner, Assessment of the Cr-B system and extrapolation to the Ni-Al-Cr-B quaternary system. *Calphad* 26, 477 (2002).
20. G.J. Zhou, Y. Luo, and Y. Zhou, Thermodynamic reassessment of the Nd-Fe-B ternary system. *J. Electron. Mater.* 45, 418 (2016).
21. L. Battezzati, C. Antonione, and M. Baricco, Undercooling of Ni-B and Fe-B alloys and their metastable phase diagrams. *J. Alloys Comp.* 247(1–2), 164 (1997).
22. B. Hallemans, P. Bellen, P. Wollants, et al., Thermodynamic reassessment of the Fe-B system and calculation of the Fe-Nd and Nd-B phase diagrams, presented at Calphad XXIII, Madison, USA, June 1994 P.12
23. G.J. Zhou, A.H. Cai, and Y. Luo, Thermodynamic assessment of the B-Nd-Cr system. *Mater. Lett.* 221, 15 (2018).
24. M.V. Chepiga, and Yu.B. Kuz'ma, Phase equilibrium in the system Chromium-Iron-Boron. *Inzvest V. U. Z. Chernaya Met.* 3, 127 (1970).
25. S. Hiroaswa and H. Kanekiyo, Nanostructure and magnetic properties of chromium-doped Fe3B-Nd2Fe14B exchange-coupled permanent magnets. *Mater. Sci. Eng. A* 217, 10284 (1996).
26. B. Hallemans, P. Wollants, and J.R. Roos, Thermodynamic reassessment and calculation of the Fe-B phase diagram. *Z. Metallkd.* 85, 675 (1994).
27. L.M. Pan, Phase equilibria and elastic module of rapidly solidified Fe-Cr-Mo-B and Fe-Cr-Ni-B alloys, Dissertation for the degree of doctor of philosophy, University of surrey, UK, 1992
28. B. Hallemans, P. Wollants, and J.R. Roos, Thermodynamic assessment of the Fe-Nd-B phase diagram. *J. Phase Equilib. Diff.* 16, 137 (1995).
29. K.H.J. Buschow, D.B. Demooij, and H.M. Vannoort, Properties of metastable ternary compounds and amorphous alloys in the Nd-Fe-B system. *J. Less-Common Met.* 125, 135 (1986).